Anti-aliasing in Aircraft Cockpit Display System Based on Modified Bresenham Algorithm and Virtual Technology

Sun Dan and Bai Jie
Tianjin Key Laboratory of Civil Aircraft Airworthiness and Maintenance, Civil Aviation University of China, Tianjin 300300, P. R. China

Shi Zhibo
Aeronautical Automation College, Civil Aviation University of China, Tianjin 300300, P. R. China

Abstract—**In this paper, an improved Bresenham algorithm is proposed in order to improve the display effect of the digital instrument display systems in aircraft and aviation simulators with following the ARINC 661 specification. According to the algorithm, the pixel brightness is calculated according to the proportional relation of the distance to the pixel for realizing the anti-aliasing. In Combine with areal sampled and double buffer image processing technology, the idea can increase the operation efficiency compared with the traditional method. In accordance with the analysis of the ARINC 661, the air data system instrument is implemented in the VAPS. Experimental results reveal that the improved algorithm and digital image processing technology can indeed solve display distortion problems more effectively and accurately, the display effect is improved obviously. The implemented schemes can achieve the airborne electronic display system on the high performance and satisfy aircraft airworthiness requirements and standards.**

Index Terms—**Virtual Digital Avionics Instrument System; Anti-aliasing; Improved Bresenham algorithm; VAPS; ARINC 661**

I. INTRODUCTION

The avionic instruments in the cockpit display system (CDS) is very critical to the pilots, because they will gain the aircraft integrated information from these devices. The numerical and graphical image information will be shown on the system. The cockpit display system merges the many of the parameters sent by the sensors to display the aircraft components parameters. Rather than the flight deck instrumentation and control devices, a high fidelity visual, aural, and motion cueing system are cued to pilots [1]. Therefore, whether the avionics display perfectly is a very important issue in the aircraft and the aviation simulators to the operator. When the distortion phenomenon happens, such as jagged edges, inaccurate calibration and so on, the wrong information may influence the pilots' judgment and result in the wrong control to the aircraft, even an air crash happens. With the development of aeronautical instruments design visualization, software test tools and computer graphics etc, the digital instruments are replacing the traditional mechanical instruments, which make the avionic instruments system have the characteristics of flexibility, low cost, easy to transplant and short development cycle etc [2, 3].

Pixels are distributed in the dot-matrix liquid crystal displays (CRD). Some distortion will appear due to the graphics are constituted by a series of same luminance pixels when drawing non-horizontal and non-vertical line or polygon boundary on the CRD. This distortion is called aliasing which is caused since the discrete used to state the continuous quantity. The technology which is used to eliminate distortion is called anti-aliasing. In the anti-aliasing area, the most popular two approaches include [4]: Weighted area sampling and improve resolution. The first is constrained by the display hardware and the cost and hardly to be realized; the second utilizes human visual characteristics to Obtain better visual effect through the modified algorithms.

Gouthas E T et al. [5] proposed to use zoom anti-aliasing (ZAA) procedure for rendering computer-generated targets at long range. Point source targets can be successfully conserved by the theory. The approach didn’t consider the straight and other graphics.

Liu Tao et al. [6] proposed a cone filter anti-aliasing idea for drawing straight line. However, the algorithm has complex computational which is not conduce to the application.

Jia Y L et al. [7] proposed a modified Bresenham algorithm to draw the straight efficiently, but the algorithm had not to consider the effect of the pixel luminance to the system.

MS Saleem et al. [8] appreciated the efficiency of Bresenham algorithm and extended this concept to 3-D linear and helical movement in CNC machines.

Zhang H et al. [9] proposed a fast algorithm by using approximate pixels to render the straight; the experiment proved that the time was saved compared with other algorithm. Unfortunately, the real vision effect of simulation, animation and visualization was not given in the paper.

Kumar S. Ray et al. [10] proposed an algorithm for line drawing using parametric equation. There were two

doi:10.4304/jmm.9.6.765-773

algorithms presented in the paper, one used the floating-point arithmetic and the other used integer arithmetic, the proposed algorithms reduced the number of lines of code and computationally become more efficient, but the visualization was not given as paper [9].

From the existing literatures on anti-aliasing, we know that although various anti-aliasing algorithms have been proposed to be used in the display system, they have one main drawback, the two methods are not consolidated together, and especially electronic display hardware has made significant progress now. Hence despite the fact that current researches on algorithms modification have made a great progress, the display effects and the display efficiency still need to be improved.

As we know, the design of instrument display systems will cost large amounts of capital of electronic equipment manufacturers; however, the design still is a long development cycle. Therefore, it is greatly significant to apply virtual visual technology in the early phase of instrument design [11], which can improve the design level, reduce the cost and shorten the cycle.

ARINC 661 Specification is proposed for the industry system to make the CDS standardization by American Airlines Radio Association in 2001. The CDS and the avionics equipments (user application, UA) are separated in the specification. In the recent years, the new generation CDS , which follows the ARINC 661[12], is a widely used in the active matrix liquid crystal display (AMLCD) multifunction display based on the Virtual Technology, such as in the U.S. F-22, B-777, A380 and the French Rafale etc.

Rouwhorst W et al. [13] had developed and evaluated the an Integrated Situation Awareness System in the CDS following the ARINC 661 Specification, and described the results of 2005 piloted experiment through two airlines crew. The conclusion suggested that strategic oriented safety systems in flight simulators should be advocated.

Verhoeven R et al. [14] proposed a prototyping interactive cockpit applications technology to increase the flexibility of the prototyping process. The ability had been proved to be very effective and the application domain possibility had been broadened.

Tankeu-Choitat A et al. [15] described the context of future large aircraft interactive cockpits and designed self-checking widgets which used interactive cooperative objects (ICO) according to the ARINC 661 standard, but there was not related simulation experiments.

Liu J et al. [16] had the analysis to the ARINC 661 specification and simulation for the Primary Flight Display (PFD) panel, but in his work, data interchange in the whole CDS was not realized, the dynamic display effect was not given.

In the contribution, a modified Bresenham anti-aliasing algorithm is proposed to solve the display distortion problems in the CDS, such as the serration and step-form of the straight lines. The modified algorithm can overcome the shortcoming of the traditional Bresenham algorithm through the pixel brightness to be adopted by the distance proportional relation to the adjacent pixel, and then improve the visual effect. Furthermore, the double-buffering and area sampling technology are adopted to obtain the best design effect of the virtual digital avionics instruments (VDAI) based on VAPS software. In the design and simulation process, ARINC 661 specification is analyzed and implemented.

The rest of this paper is organized as follows. In Section II, Modified Bresenham algorithm and the theoretic foundation of the study are described. In Section III, we explain ARINC 661 Specification, where the standard procedure and technical plan design are presented. The last part of section is devoted to show experimental results. Finally conclusions are drawn in Section IV.

II. Improved Rendering Algorithm of the VDAI

As described above, there are two major problems in the process of drawing Aviation Instrument in the CDS. One is the “aliasing”, which refers to the phenomenon of serrated deformation or saw tooth in the screen with real-time rendering graphics. The distortion is caused due to display by a series of discrete on the computer, namely, a set of the brightness of the dots (pixels). Serious aliasing will make graphics out of shape. If the instruments have serious aliasing, that will cause the pilot's misjudgment, which will result in the adverse consequences. So the severe aliasing should be avoided in rendering the graphics of the instrument graphics in the computer, some methods must be used to eliminate or reduce the aliasing, such as Bresenham algorithm, Wu algorithm and cone filter algorithm etc.

The other is that how to obtain real-time graphic rendering for the real-time data, and how to solve the display problem such as flicker because screen stagnation and blinking which often occur intermittently when the instrument is operating. Generally, to solve the above problem and further improve the display effect of the CDS, some measures could be used:

(1) A method to increase the sampling points closes to or reaches the need of the sampling theorem for the display resolution improvement.

(2) After having the sample in the actual graphics processing, post-processing before the instrument display.

(3) A better two-dimensional function is selected in the process to eliminate the noise.

(4) Double-buffering technology should be adopted in software design.

Straight line segment is one of the most basic graphs in airborne display system. The generation efficiency and display quality of straight line segments will have direct impact on the whole system. A modified algorithm is proposed base on Bresenham algorithm in line drawing, which is combined with the symmetry of the geometric figure and the control to the brightness of the pixels.

Bresenham algorithm principle is introduced simply as shown in Fig. 1. In order to facilitate discussion, the linear slope k is assumed between 0 and 1.

The linear slope can be set as

$$k = dy/dx \tag{1}$$

And the starting point coordinate is $(0,0)$ in the coordinate axis, because $0<k<1$, when x-axis increases 1 unit to the right, y-axis will increase k unit. And two pixels will be met in the next step. One pixel is $(1,0)$ and the other is $(1,1)$. Which pixel should will be lit will be depend on the distance of the pixel to the line.

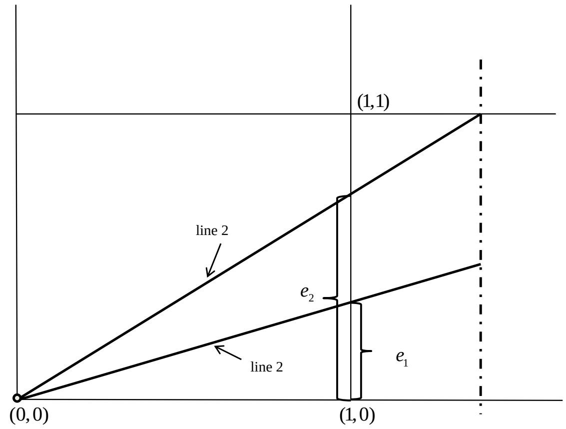

Figure 1. Bresenham algorithm schematic

For the line 1, if $e_1<1/2$, the pixel $(1,0)$ will be brighten. For the line 2, if $e_2>1/2$, the pixel $(1,1)$ will be brighten. After each one pixel along the x-axis forward, then to compare the y-axis incremental value, the brighten pixel will be the point which the closest by a straight line. According to this selection strategy, the line can be completed by a series of pixels. As seen from the above principle, the Bresenham algorithm will make a straight line produce jagged boundaries although it is simple and efficient, which is shown in the Fig. 2.

In the next, a modified algorithm will be proposed to achieve anti-aliasing which makes use of the multi-segment similarity in a line segment. It is combinated with the symmetry of the geometry based on the generally Bresenham algorithm. This approach avoids duplication operations, improves the speed of anti-aliasing and time-saving anti-aliasing.

Assuming the linear equation in the plane is:

$$y=kx+b \tag{2}$$

where k is the slope, b is the intercept. The plane straight line can be divided five classes according to the range of the slope:

1) $0<k<1$;
2) $1<k<\infty$;
3) $-\infty<k<-1$;
4) $-1<k<0$;
5) $k=0,|k|=1,|k|=\infty$;

According to the characteristic of the digital graph, the fifth class needn't the anti-aliasing when draws the straight. For the second, third and forth, they can be gained and drawn by means that to change the slope sign or the position of the function variable x and y. So we only need have the discussion to the first situation.

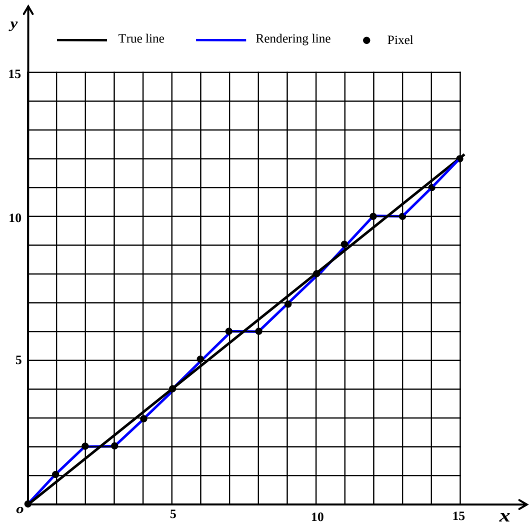

Figure 2. The Rendering line based on Bresenham algorithm

For straight line l, its endpoints are (x_0,y_0) and (x_n,y_n) respectively. We may assume the situation which is $x_0<x_n$, $y_0<y_n$ as well.

Now defining

$dy=y_n-y_0$, $dx=x_n-x_0$,

Because $0<k<1$, we can confirm that

$0<dy<dx$

Noting $m=gdc(dx,dy)$, where m is greatest common divisor of dy and dx.

The equation (1) can be written as

$$k=\frac{dy}{dx}=\frac{m\cdot q}{m\cdot p}=\frac{q}{p} \tag{3}$$

where p and q are relatively prime positive integers. As shown in the Fig. 3, from the description above, we can get

$m=gdc(15,12)=3$, $p=5$, $q=4$.

For the modified Bresenham algorithm, we have two conclusions to be stated in the next, which can help improve the image processing efficiency more obviously.

Conclusion1. For a straight line l, its pixels sequence is $\{(x_i,y_i)|i=0,1,2,\cdots,n\}$, which can be divided into m segments: l_1, l_2, l_3, $\cdots$, l_m and the end pixel. So there are p pixels in each segment and the first pixel falls on the straight line l accurately. Furthermore, only $m+1$ pixels do that in the entire sequence.

Proof. From the equation (3), dx can be reduced

$$dx=x_n-x_0=mp \tag{4}$$

There are $m+1$ pixels in the entire sequence. As shown in the Fig.3, the pixels sequence can be divided into m segments: l_1, l_2, l_3, $\cdots$, l_m and there are p pixels in each segment.

Assuming the j_{th} segment starting point is (x_{ij}, y_{ij}), $0 < j < m$. The x-axis coordinate value is given

$$x_{ij} = x_0 + jp \tag{5}$$

Furthermore,

$$\begin{aligned} k &= \frac{y_{ij} - y_0}{x_{ij} - x_0} \\ &= \frac{k(x_0 + jp) + b - y_0}{(x_0 + jp) - x_0} \\ &= \frac{kx_0 + b - y_0 + kjp}{jp} \end{aligned} \tag{6}$$

So the first pixel (x_{ij}, y_{ij}) falls on the straight line l accurately.

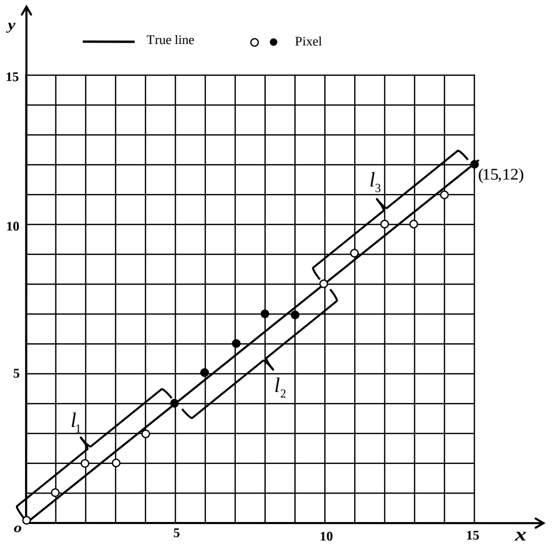

Figure 3. Schematic of modified Bresenham algorithm

The y-axis coordinate value is given

$$y_{ij} = y_0 + jq \tag{7}$$

The height of each segment follow the y-axis is q. Because

$m = gdc(dx, dy)$

So $m+1$ pixels, which contain the end point, fall on the straight line l accurately in the entire sequence. For the points that don't fall the line, as point A shown in Fig. 4. Two pixels are drawn on each side of the line segments. Actual brightness of each pixel is multiplied by a weight as to draw the color brightness.

It is can be assumed that the brightness of a pixel is Θ, the distance that from point A to pixel A1 is h_1 and the distance that from point A to pixel A2 is h_2. In order to gain the satisfied display effect and eliminate the distortion visually, the brightness of pixel A1 is $h_2\Theta$ and the other is $h_1\Theta$, where $h_1 + h_2 = 1$, $0 \le h_1 \le 1$, $0 \le h_2 \le 1$. Different from the general Bresenham algorithm, the line segments all will be drawn with the different brightness pixel, which can improve the generation speed and quality of the straight line and implement in FPGA easily. According to the brightness, serrated deformation will be improved.

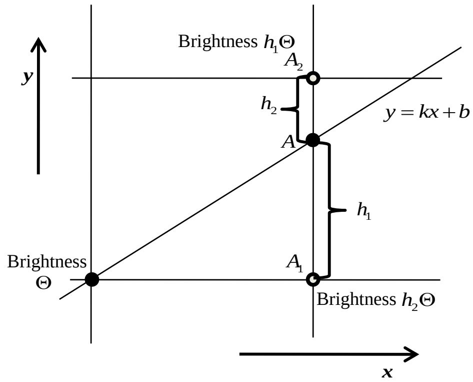

Figure 4. Draw line in improved Bresenham algorithm

Conclusion2. For a straight line l, its pixel sequence is $\{(x_i, y_i) | i = 0,1,2,\cdots,n\}$, the coordinate value y in the sequence is symmetrical relative to the midpoint of the straight line l, namely,

$$y_{n-i} = y_n - y_i + y_0, (i = 0,1,2,\cdots,\left[\frac{n}{2}\right]),$$

where $\left[\frac{n}{2}\right]$ means the integer.

Proof. Because the equation

$$x_i = x_0 + i \tag{8}$$

So we can get the equation

$$\begin{aligned} y_i &= kx_i + b \\ &= k(x_0 + i) + b \\ &= y_0 + ki \end{aligned} \tag{9}$$

where $i = 0,1,2,\cdots,n$.

Therefore, the equation (9) can be used in the next equation

$$\begin{aligned} y_{n-i} &= kx_{n-i} + b \\ &= k(x_n - i) + b \\ &= y_n - ki \\ &= y_n - y_i + y_0 \end{aligned} \tag{10}$$

where $i = 0,1,2,\cdots,\left[\frac{n}{2}\right]$.

When slope k has the other value range, for example the slope $k \in (1,\infty)$, the method that to change the variable x and y will make the slope $k \in (0,1)$, which does the rest of the situations. According to the conclusion 1 and conclusion 2, the aliasing situations and rendering speed will get an excellent improvement. The rendering efficiency of drawing a line is improved with computation reduction. When the line l_1 is completed, the other segments will be drawn by copying l_1 based on the segments similar characteristics.

According to the above conclusions, the anti-aliasing technology that based on improved algorithm has obvious advantages to the general. Because the pixels amount needed in this algorithm only are half of the dx at the most. If $m > 0$, $dk = 0$ will be apparent after dx/m pixels are calculated. If there is not pixel falls on the straight accurately when the calculation up to the half of dx, the situation $m = 1$ will be ascertained, so we can have the symmetry copy operation.

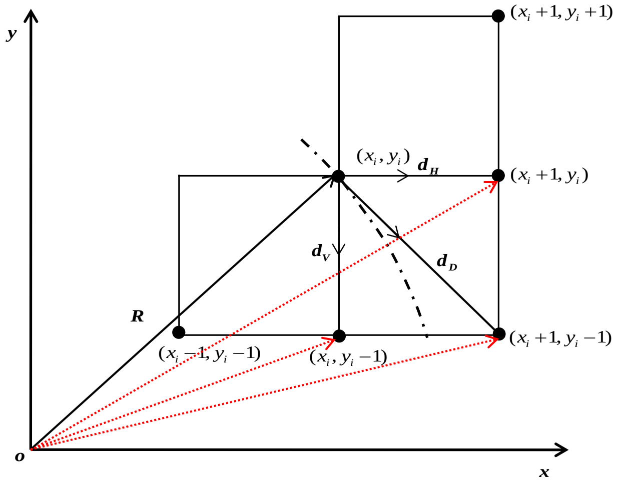

Figure 5. Positional relationship between the circle and the grating grids

Circle is another one of the most basic graphs in airborne display system. As shown in the Fig.5, the quarter of a circle is drawn in the first quadrant, which radius is R, because of its symmetry.

Assuming the center of the circle is at the origin and the pixel. Point (x_i, y_i) on the circle is the pixel dot. When circle generating clockwise, the next pixel only to chose the points (x_i+1, y_i), (x_i+1, y_i-1) and (x_i, y_i-1).

Defining as the following:

$$d_H = \left|(x_i+1)^2 + y_i^2 - R^2\right| \tag{11}$$

$$d_D = \left|(x_i+1)^2 + (y_i-1)^2 - R^2\right| \tag{12}$$

$$d_V = \left|x_i^2 + (y_i-1)^2 - R^2\right| \tag{13}$$

where d_H, d_D and d_V denote the absolute values of the square of the distance from these points to the circle. The minimum among them will be selected to be drawn. Therefore, we have the definition

$$D_H = (x_i+1)^2 + (y_i-1)^2 - R^2 \tag{14}$$

The position of the point (x_i+1, y_i-1) can be judged by the D_H value. If the $D_H < 0$, the point (x_i+1, y_i-1) will be in the circle, otherwise out.

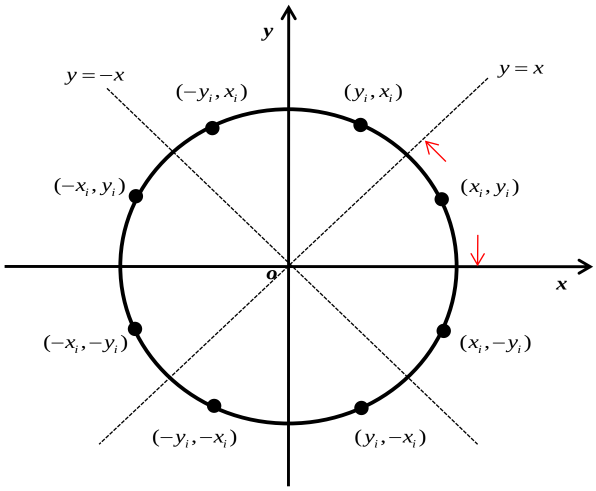

Figure 6. Eight symmetry of the circle

When the point inside the circle, we must decide which point should be chosen between point (x_i+1, y_i) and point (x_i+1, y_i-1).

So we have the equation

$$\delta_{HD} = d_H - d_D$$
$$= \left|(x_i+1)^2 + y_i^2 - R^2\right| - \left|(x_i+1)^2 + (y_i-1)^2 - R^2\right|$$

If $\delta_{HD} \le 0$, the point (x_i+1, y_i) will be selected, otherwise the other.

When the point is outside the circle, we have the equation

$$\delta_{VD} = d_V - d_D$$
$$= \left|x_i^2 + (y_i-1)^2 - R^2\right| - \left|(x_i+1)^2 + (y_i-1)^2 - R^2\right|$$

If $\delta_{VD} \le 0$, the point (x_i, y_i-1) is selected, otherwise the other. The lower right pixel is preferential to be chosen in the process, and similar to other cases.

For any circle, its center can be moved to the origin in the axis. Taking into account the circular symmetry as shown in the Fig.6, only one in eight arcs is needed to be drawn. When the anti-aliasing of one in eight arcs is completed, the whole circle also will be done. The one in eight arcs can be divided into many line segments, so the aliasing problem can be solved by the line anti-aliasing technology.

III. Design and Simulation of VDAI Based on VAPS

In the section, the ARINC661 specification will be introduced and we have application analysis about it in order to design the instrument. The instruments should be developed following the flow chart in the VPS as shown in the Fig. 7.

ARINC 661specification structure can be divided into two phases on the time, which are the definition phase and run-time phase. It can be divided into UA and CDS according to the function. The information exchanges follow the A661protocol between UA and CDS, which can weaken the coupling between them and improve the maintenance and repeatability of the system. The standard system structure is shown in the Fig. 8.

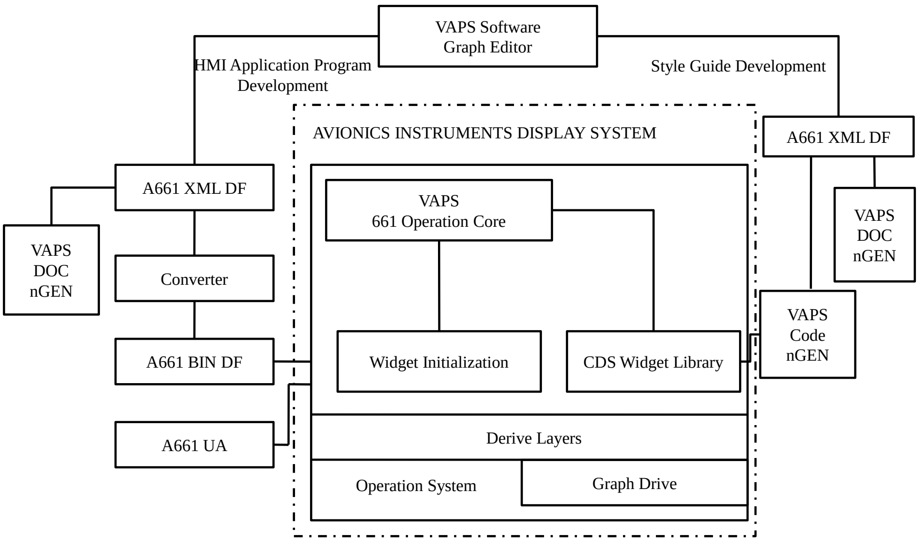

Figure 7. Flow chart of abided by ARINC 661 in the VAPS

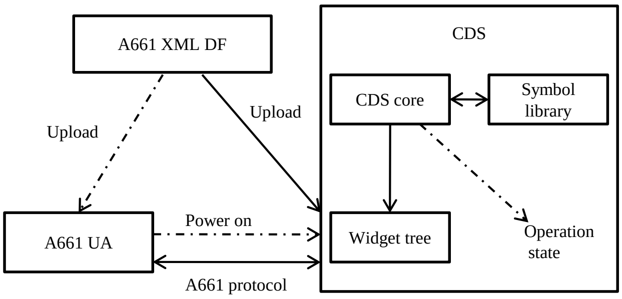

Figure 8. ARINC 661 standard system structure

In the specification, CDS is used to show the widget in real-time. Widget employs the layer architecture and the same widget can be used in different layer as well. Every window can display multiple different layers which are constituted by widget parts. All the logic processing of the CDS will be operated in the UA, It mainly includes two aspects: one is to provide the updated data for the CDS, and the other is to have the logic judgment and response to the user's operation. UA can be realized in various programming language and designing skills. Widget recognition is the base of the communication between UA and CDS as shown above. There are 42 species widgets, which belong to 6 classes, in the ARINC 661.UA can verify the unique widget through tag format [UAID][LayerID][WidgetID].

When the CDS is designed in the initial phase following the ARINC 661 through the above analysis, the CDS should satisfy:

1) The XML definition file (DF) can be established in a XML format;
2) The BIN DF can be established in a binary format;
3) Widget library can be established;
4) The CDS display environment can be established;
5) The CDS should be compatible with the subsequent amendments and supplement function of ARINC 661.

In the design procedure of the avionics, the safety and reliability are crucial. So the safety certification standards DO-178C must be complied strictly. The Altimeter and Mach are taken as an example to introduce design and simulation in VAPS software abided by the ARINC661 specification. The anti-aliasing and optimization technology with the improved Bresenham algorithm has been applied and implemented. In the Fig.9, Design and implementation schematic of CDS is given follow basic ARINC661.

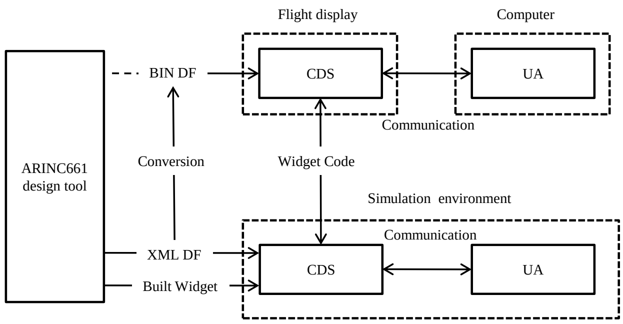

Figure 9. Schematic of CDS follow the ARINC 661 standard

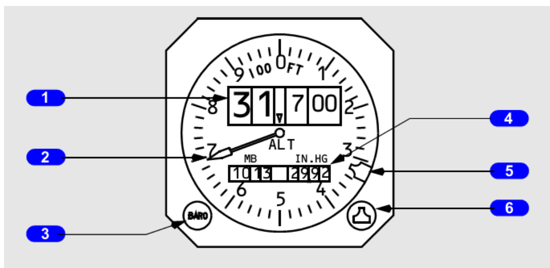

Figure 10. The Altimeter diagram of B737-300

The size, shape and behavior of the digital virtual avionics instrument (DVAI) should be the same as the real aircraft instrument. Only that, the DVAI is able to accurately reflect the design requirements and the effect. Therefore, it should be familiar with the basic components of the avionics instrument before drawing by the designer. As shown in the Fig.10, it is the block diagram of the basic components of the B737-300 cockpit altimeter. The Num.1 is the digital counter in the instrument. Num.2 is height pointer, Num.3 points to the pressure setting control button and Num.4 to pressure setting window, Num.5.is reference height mark and Num.6, which is reference height mark control button. Above that, we can have the layout of the avionics [17].

According to Fig. 10, the layout is designed and the instrument is drawn in the VAPS which is shown in the Fig. 11. The layout can be saved as the '*.FRM' file. Select the project, run the virtual instrument to test if the appearance meets the requirements [18, 19, 20].

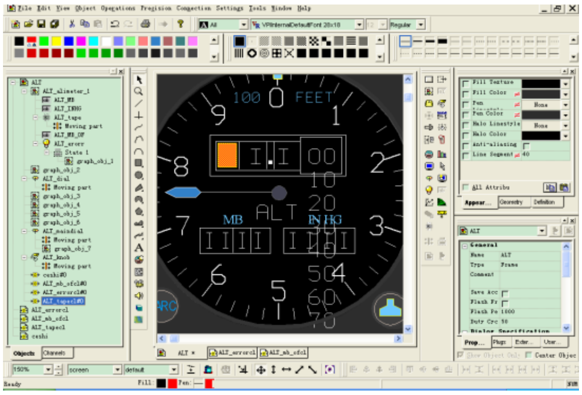

Figure 11. The workspace of the Altimeter layout

The outward appearance of the avionics is only completed when connect the instrument layout part, which is to give the model defined plug-ins and make the plug-ins with the corresponding data channel connection. [21-22]. The data channel is the structure to cache data and the exchange link between input and output components. The data, from the channel to the plug-ins, make the parts do the corresponding movement in accordance with pre-set trajectory of the moving parts, which is shown in Fig. 12. Window will have the check that if the connection is correct by clicking on the drop-down list in the Window menu and docking.

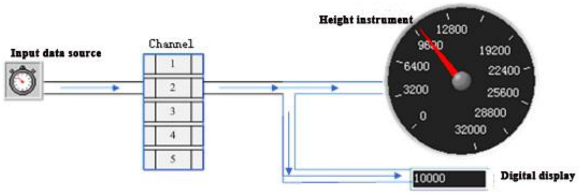

Figure 12. The data channel between input and output

There are two behavior models in VAPS application : one is the finite state machine (FSM) and the other is augmented transition network (ATN). Discrete input of the FSM is called the "event" is a very effective model. FSM is a nonlinear model which is very useful in building an interactive system and interface.

ATN is built on the basis of FSM, which is not only composed of a series of states and events but also conversion arcs. The difference is that it is needed to increase the action response in the ATM. This was reflected in three aspects:

(1) The transition to the new state by the test conditions,

(2) The implementation of response can be to achieve some desired functionality on the transfer arc,

(3) The ATN model adds a discrete output (response) corresponds to FSM model in discrete input (events).

FSM model and ATN model are shown in Fig. 13.

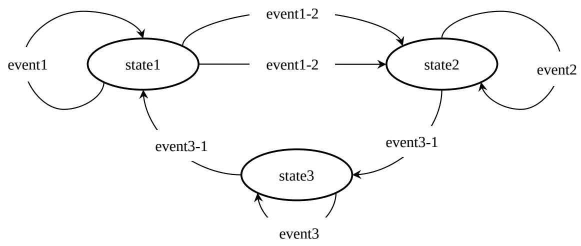

(a) FSM model in VAPS

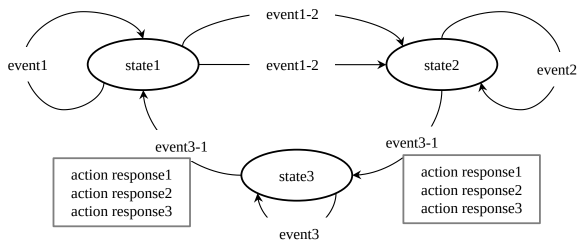

(b) ATN model in VAPS

Figure 13. The two models: FSM and ATN

The aforementioned framework can be loaded in the initialized state when ATN model is designed in Mach.There are two ways in constructing ATN model: one is the use of external C programming and the other is to fill in the data table in ATN status bar, then to generat ANSIC code.

In order to get better display effect, the improved Bresenham algorithm should be implemented in the program to suppress the aliasing and improve the computational efficiency. But beyond that, double-buffering technology is also used in VAPS to eliminate screen flicker and stagnation. Double-buffering technology is the operation in memory (not visible cache) firstly, and then the operating results copied to the screen memory (visible memory) display technology. In the VAPS graphics redraw the system, two buffer exchange time is an integer multiple of the system screen refresh cycle. So for this reason, no extra draw when redraw is necessary to choose, which reduces the number of graphics redraw. In the process, the interface design should be abided by the ARINC Specification 661. Some measures, such as run the test module, dynamic, graphical HMI real-time interaction, should be adopted to improve the instrument.

In the paper [23, 24, 25], which reveal that when the instrument have been running in the PC environment, the anti-aliasing effect will be more obvious, which is shown in Fig. 14.

The virtual digital avionics instruments (VDAIs) are connected in VC++ to constitute a complete system. Atmospheric data parameters in the flight simulator system achieve the simulation of the entire process. And have the entire system's functional and performance testing to achieve good results. Fig. 15 shows the instrument part of the operating interface.

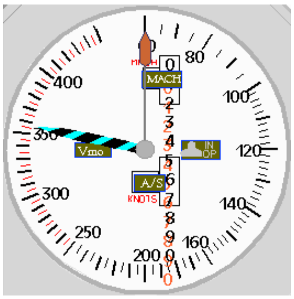

(a) The Mach display effect before Anti-aliasing

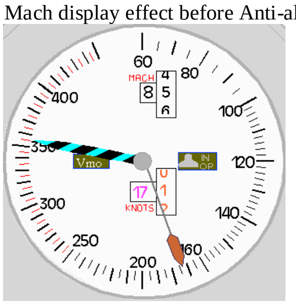

(b) The Mach display effect after Anti-aliasing

Figure 14. The compare of display effect in VAPS

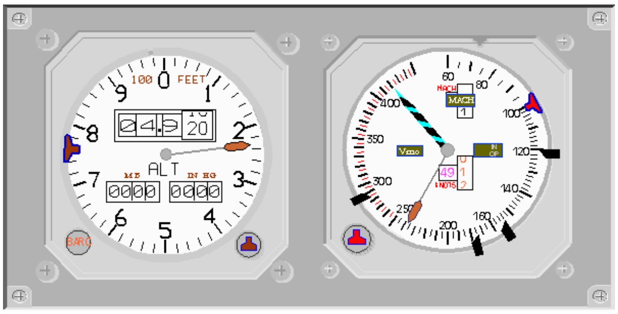

Figure 15. The instrument part of the operating interface

IV. Conclusions

This paper derived and validated an improved Bresenham algorithm for the air data system of the cockpit display system in VAPS software. The modified algorithm can reduce the calculation, improve drawing efficiency and enhance display effect integrating with area sampling technology and double Double-buffering technology. The work can eliminate the distortion and serrate deformation generated by the characters and lines, and obtains the desired real-time display images. In the design procedure, ARINC661 Specification is analyzed and the structure of the CDS is given following the standard. The process of debugging and simulation reveals that the modified Bresenham algorithm, area sampling and double-buffering technology can be able to achieve the desired optimization in the VAPS for the avionics with the ARINC661 Specification.

Acknowledgment

We would like to express our gratitude to the anonymous reviewers of this paper for their helpful comments and suggestions. The work was sponsored by Research Funds for the Central Universities Basic Fund of China (Grant No.3122013D012).

References

[1] Matthew W. Blake. “The NASA Advanced Concepts Flight Simulator-A unique transport aircraft research environment”, *AIAA Meeting Papers on Disc*. 1996, pp. 385-392.

[2] George A. Geri, Marc D. Winterbottom. “Effect of display resolution and antialiasing on the discrimination of simulated-aircraft orientation”, *Displays*, 26(4), 2005, pp. 159-169.

[3] Neal Fennell, Shane Hemmens, “Miles Moody. Engineering Flight Simulator Designed for Human in the Loop Interaction”, *Proceedings of the SETE2000 Conference*, 2000, pp. 8-10.

[4] YANG L, ZHAO M, FENG C, et al, “Anti-aliasing in Aircraft Cockpit Display System”, *Chinese Journal of Liquid Crystals and Displays*, 2006, 6: pp. 018-021.

[5] Gouthas E T, Williams O M, “Real-time zoom anti-aliasing improvement using programmable graphics processing units Defense and Security Symposium”, *International Society for Optics and Photonics*, 2006: pp. 620814-15.

[6] LIU T, GAO Q, ZHAO G, “A New Antialiasing Technique for Drawing Straight Line Based on Cone Filter”, *Journal of Engineering Graphics*, 2006, 3, pp. 010-013.

[7] Jia Y L, Zhang H C, Jing Y Z, “A modified Bresenham algorithm of line drawing”, *Journal of Image and Graphics*, 2008, 13(1), pp. 158-61.

[8] Saleem M S, Saleem M M, “Bresenham type fast algorithm for 3-D linear and helicalmovement in CNC machines”, *WSEAS Transactions on Systems*, 2004, 3(4), pp. 1548-1554.

[9] Zhang H, Zhu C, Yang J, “Fast algorithm for line rasterization by using slope 1”, *Autonomous Decentralized Systems*, ISADS 2005. Proceedings. IEEE, 2005, pp. 508-512.

[10] Ray K S, Ray B K. “An algorithm for Line Drawing Using Parametric Equation”, *International Journal of Computer Graphics*, 2011, 2(1), pp. 9-16.

[11] Liu Jian, Liu Qin, Sun Yongrong etc, “Research on ARINC 661 Specification and Its Application Development”, *Computer and Modernization*, 2010. 4, pp. 188-192.

[12] ARINC. ARINC661Specification: Cockpit Display System Interfaces To User Systems. *Aeronautical Radio INC*, 2002.

[13] Rouwhorst W, Marsman A. “A piloted investigation of an Integrated Situation Awareness System (ISAS)”, *AIAA Modeling and Simulation Technologies Conference and Exhibit*. 2006.

[14] Verhoeven R, de Reus A. “Prototyping interactive cockpit applications”, *Digital Avionics Systems Conference*, 2004. DASC 04. The 23rd. IEEE, 2004, Vol. pp. 2, 2: 9. A. 3-91-10.

[15] Tankeu-Choitat A, Navarre D, Palanque P, et al. “Self-checking components for dependable interactive cockpits using formal description techniques”, *Dependable Computing (PRDC)*, 2011 IEEE 17th Pacific Rim International Symposium on. IEEE, 2011, pp. 164-173.

[16] LIU J, LIU Q, SUN Y, et al. “Research on ARINC 661 Specification and Its Application Development”, *Computer and Modernization*, 2010, 4. pp. 050-053.

[17] Boeing 737-300 Maintenance Training System for the Civil Aviation Institute of China, *CAE*. 1998, pp. 120-300.

[18] Wanling-Li. “Application of VAPS Technique to Develop Multifunctional Display Software for Manned Spacecraft”, *Space Craft Engineering*. 2008, 9, pp. 20-24.
[19] Gang-Bai. Mei-Yuan, Qiong-Chen. “The Design and Implementation of Virtual Cockpit Multi Function Display”, *Aircraft Design*. 2005. 4, pp. 50-54.
[20] Qun-Kuang, Jingjin-Zhang, “The Design of Cockpit Simulated Instrument System”, *Civil Aircraft Design and Research*. 2010. 4, pp. 29-33.
[21] Boeing 747-400 Full Flight Simulator for NASA. *Volume 1. Technical Specification, TPD08593-1 Rev. 3. CAE Electronics Ltd*. Canada, June, 1992, pp. 0-258.
[22] Xiaowei-Ren, Wei-Zhang. “Study for the Evaluation Method of Flight Deck Simulation Based on VAPS”, *Humanity Ergonomics*, 2011. 3, pp. 41-44.
[23] SHI ZhiBo. “Design and simulation of virtual instrument anti-aliasing based on VAPS”, *Application of Electronic Technique*, 12. (2010), pp. 046-050.
[24] Lefebvre Y. “A flexible solution to deploy avionics displays to multiple Embedded Platforms”, *Digital Avionics Systems Conference*, DASC 2008, 5, pp. A. 3-1-5. A. 3-9.
[25] Chandrasetty V A, Aziz S M. “FPGA Implementation of a LDPC Decoder using a Reduced Complexity Message Passing Algorithm”, *Journal of Networks*, 2011, 6(1). pp. 36-45.